

Fragmentation of CH_4 caused by fast-proton impact

I. Ben-Itzhak, K. D. Carnes, S. G. Ginther, D. T. Johnson, P. J. Norris, and O. L. Weaver
James R. Macdonald Laboratory, Department of Physics, Kansas State University, Manhattan, Kansas 66506
(Received 19 October 1992)

The cross sections of the different breakup channels of CH_4 , produced by 4-MeV proton impact, have been measured using the coincidence time-of-flight technique. The relative abundances of the different breakup channels were evaluated for collisions in which the molecule broke into two charged fragments as well as for collisions where only a single charged molecular ion or fragment was produced. These relative abundances are compared to the ones measured for photodissociation and for electron and proton impact. Only the CH_4^+ ion survives long enough to be detected as a molecular ion, while the doubly charged CH_4^{2+} ion dissociates rapidly. The most probable final product of the fragmentation of doubly charged methane as formed by fast-proton impact is $\text{H}^+ + \text{CH}_2^+ + \text{H}$. The abundance of $\text{H}_m^+ + \text{CH}_n^+$ ($m + n \leq 4$) ion pairs decreases rapidly with increasing m , as suggested by Siegbahn [Chem. Phys. **66**, 443 (1982)]. The momentum of neutral fragments, in channels where they are produced, is small in comparison with the momentum of the charged fragments so that two-body breakup holds approximately. The deviation from two-body breakup increases with increasing number of neutral hydrogen atoms produced. The sensitivity of the experimental method enabled us to extend the study of the fragmentation pattern of CH_4^{2+} to include small breakup channels such as $\text{CH}_4^{2+} \rightarrow \text{H}_3^+ + \text{CH}^+$. Furthermore, some breakup channels of the triply charged CH_4^{3+} have been detected as triple coincidences.

PACS number(s): 34.50.Gb, 34.90.+q

I. INTRODUCTION

The fragmentation process of small polyatomic molecules has been investigated mostly for photoionization [1–4], electron impact [5–12], and fast-proton impact [12,13] using various methods. In most of these processes, one electron of the target molecule is ionized resulting in some dissociating states. A small fraction of the target molecules will be doubly ionized and dissociate into ion pairs. Using coincidence between the two charged fragments makes it possible to distinguish this small breakup channel from the main single ionization channel [2–4,10,11]. The fragmentation pattern of highly charged transient states of molecules has recently been studied using fast highly charged projectiles which can efficiently remove a few electrons in a single collision [14–16]. It is commonly expected that the electrons will be removed rapidly in comparison with the nuclear motion and slowly in comparison with the collision time. Thus, first a transient CH_4^{Q+} is formed which then either deexcites or dissociates. The momenta of the dissociating fragments come from the internal excitation of the transient molecular ion. Direct momentum transfer from the projectile is negligible for these fast collisions.

The fragmentation pattern of singly charged methane has been the subject of numerous studies. Some of these focused on a high-resolution measurement of the kinetic-energy distributions of the charged fragments [5–8]. Others focused on the fragmentation pattern (measuring either relative or absolute cross sections) [9–12]. The difference between the fragmentation pattern produced by electron impact or proton impact at the same collision velocity has been discussed by Wexler [12] and by Malhi *et al.* [13], who found in general good agreement between the two.

The fragmentation pattern of doubly charged methane, which is the molecule of interest in this work, has been studied since the early work of McCulloh, Sharp, and Rosenstock [10]. In their work the ion pairs produced by 1-keV electron impact have been measured in coincidence, and their abundances relative to the $\text{H}^+ + \text{CH}_3^+$ breakup channel have been evaluated. Similar measurements for 10-keV electron impact have been done by Backx and Van der Weil [11] which show a somewhat similar fragmentation pattern. The differences between the two measurements, namely, a higher rate of breakup channels in which more hydrogen fragments were produced for the 10-keV measurement, have been attributed to *K*-shell ionization which is possible for that case. The photodissociation fragmentation pattern, studied by Fournier *et al.* [4], shows a faster decrease in the abundance of breakup channels with an increasing number of hydrogen fragments removed. Theoretical work by Siegbahn [17] suggests that the probability of CH_4^{2+} breakup into ion pairs, $\text{H}_m^+ + \text{CH}_n^+$ ($m + n \leq 4$) will decrease with increasing m , i.e., more CH bonds breaking.

The formation and mean lifetimes of doubly charged CH_4^{2+} molecular ions and doubly charged CH_n^{2+} fragments have been of increasing interest in the past few years. Most of the studies of these long-lived molecular ions are done by charge stripping of a singly charged CH_n^+ in a single collision with various targets [18–20]. Gray, Legg, and Needham [16] reported evidence of formation of doubly charged, as well as triply charged, CH_n molecular ions in $\text{F}^{4+} + \text{CH}_4$ collisions at 1 MeV/amu. Even though some long-lived states of doubly charged methane ions have been detected, most of these ions dissociate rapidly into ion pairs.

In this paper we report the studies of methane fragmentation caused by 4-MeV proton impact. The coin-

coincidence time-of-flight (CTOF) technique and the experimental apparatus used for these studies have been described in detail elsewhere [21]. The experimental method is discussed briefly in Sec. II. Our work has focused on the determination of the relative importance of the different breakup channels for both singly and doubly charged methane. In order to accomplish this goal the relative abundance of all breakup channels and the kinetic energy released in each channel were determined. The evaluation of the relative abundances is presented in Sec. III. The main fragmentation channels of singly and doubly charged methane, and the pathways leading to them, are discussed in Sec. IV.

II. EXPERIMENTAL METHOD

Our experimental setup has been described in previous publications and will thus only be outlined briefly here (see Fig. 1). A bunched beam of protons was accelerated in the J. R. Macdonald Tandem Van de Graaff accelerator to an energy of 4 MeV. The collimated beam was then directed into a target cell containing methane gas. Pressure in the cell was kept below 0.1 mTorr to insure single-collision conditions. Ions produced in the cell's collision region were extracted and accelerated by uniform electric fields and allowed to drift into a large chevron microchannel plate detector (MCP). The times of flight of all ions hitting the detector were then recorded by a LeCroy 4208 multihit time-to-digital converter (TDC). The time reference for this measurement was a fast timing signal synchronized to the beam bunch.

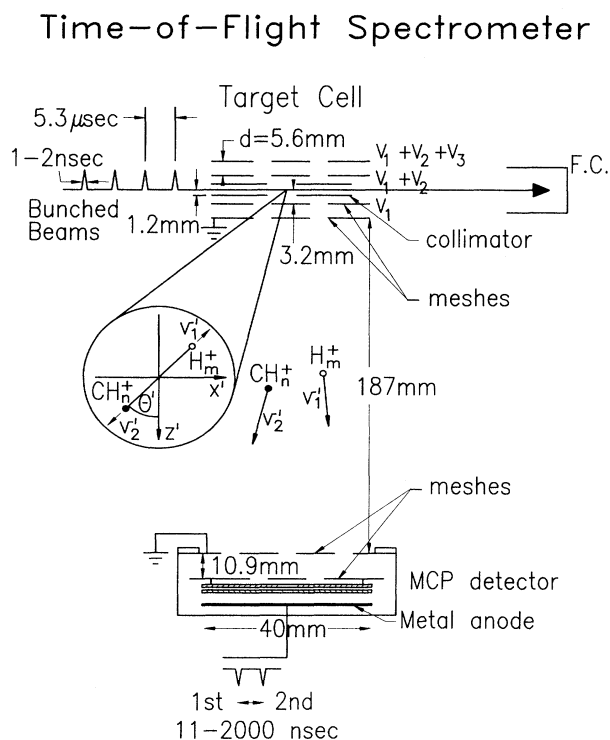


FIG. 1. The experimental setup used for coincidence time-of-flight spectroscopy. (The target cell is symmetric about the beam axis.)

Several factors had to be taken into account in order to maximize the performance of our time-of-flight spectrometer. First, the ratio of spectrometer voltages had to be correctly set to optimize time resolution. That resolution $\Delta t/t$ for the CH₄⁺ molecular ions, which typically have thermal energies (~ 0.04 eV) in these collisions [6], was found to be about 4×10^{-3} . Second, the effects of angular discrimination had to be taken into account. These were minimized by using a large exit collimator, a large detector, and strong extraction fields, but we still had to pay special attention to the light H⁺ and H₂⁺ ions. These ions have a large dissociation speed even at the typical energy of a few eV measured in the dissociation of doubly charged CH₄. Third, the discriminator level of the constant-fraction discriminator (CFD) producing the recoil signal needed to be set low enough to ensure that the singly charged CH₄⁺ ions, which have a relatively small signal, were not lost. This was verified by measuring the relative yields for single and double ionization of He atoms by fast protons and comparing to previous measurements by Knudsen *et al.* [22]. Finally, we had to consider possible losses in signals caused by first and second hits arriving too close together. The minimum separation time needed by the electronics was 20 nsec, which is less than the time difference for most first and second particles. Only coincidence events between H⁺+H⁺ and H₂⁺+H₂⁺ might have been lost after the signals were produced. These special cases will be discussed later in the paper.

III. DATA ANALYSIS

A typical spectrum of events in which only a single recoil ion was detected from the collisions of 4-MeV H⁺ and CH₄ is presented in Fig. 2. It can be seen that the main recoil ion is the singly charged methane molecule while the CH₃⁺ is the main fragment coming from the dissociation of CH₄⁺ into CH₃⁺+H. The H_m⁺ peaks

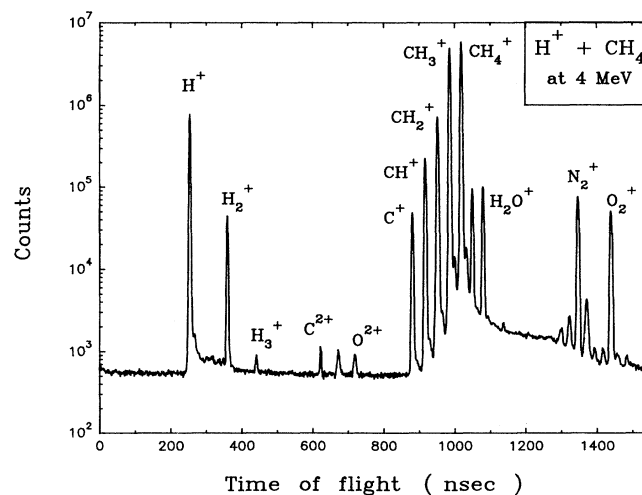


FIG. 2. TOF single-ion spectrum of methane fragmentation, produced by 4-MeV proton impact, measured with a strong extraction field of 1250 V/cm.

are much broader than the CH_n^+ peaks due to their larger dissociation speed. The ionization cross section for these collisions is small [13] (of the order of 10^{-17} cm^2) and the double-ionization cross section is expected to be much smaller. Thus, the rate of ion pairs produced from the dissociation of CH_4^{2+} is much smaller than the rate of ion and neutral species coming from the dissociation of CH_4^+ . The ion pair channels can still be determined because of the coincidence condition fulfilled by both ions hitting the detector. A typical ion-ion coincidence spectrum is shown in Fig. 3 as a three-dimensional (3D) plot of intensity versus t_1 and t_2 , where t_1 and t_2 are the times of flight of the first and second fragments, respectively. A few breakup channels measured in coincidence are identified on the figure by their times of flight t_1 and t_2 .

The number of counts in each coincidence and single-fragment peak is proportional to the production cross section of the relevant breakup channel. The efficiency for detection of both fragments in coincidence, ϵ_{mn} , and the efficiency for detection of a single ion, ϵ_r , for our time-of-flight spectrometer were discussed in detail in previous publications [21,23]. The ion-pair detection efficiency is given by $\epsilon_{mn}(E_k) = \eta_{mn} \epsilon_r^2$, where the ion-pair extraction probability, η_{mn} , depends on the kinetic energy released in the dissociation and thus must be evaluated for each breakup channel. The kinetic-energy distribution of each breakup channel was evaluated using a method commonly used in photoion-photoion coincidence (PIPICO) measurements [2-4]. In this method the time-difference spectrum, measured with a weak extraction field of 187 V/cm, is fitted with a simulated spectrum produced by an ion pair whose kinetic energy has a Gaussian distribution around \bar{E}_k , as shown in Fig. 4 for the $\text{H}_2^+ + \text{CH}_2^+$ breakup channel. The breakup energy was about 6-7 eV for the main breakup channels in agreement with the values obtained by Fournier *et al.* [4] in their studies of dissociation caused by photoionization.

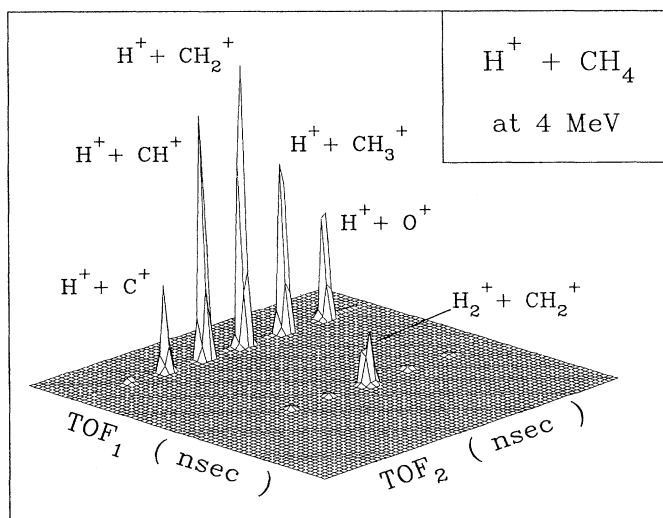


FIG. 3. Coincidence TOF spectrum of methane fragmentation, produced by 4-MeV proton impact, measured with a strong extraction field of 1250 V/cm.

The ion-pair extraction probability is not changing much over this energy range as can be seen from Fig. 5 and is approximately unity because of the small energy release. This makes the study of the fragmentation of CH_4 easier than molecules for which the energy release is large [23,24].

In most ion-pair breakup channels more than two fragments are produced, for example, the main breakup channel $\text{CH}_4^{2+} \rightarrow \text{H}^+ + \text{CH}_2^+ + \text{H}$. The Coulomb repulsion between the ion pair is expected to be stronger than that between the ion and neutral fragment. Thus, neutral fragments are expected to have small momenta relative to the charged fragments. This can be seen from the small dissociation energies measured for single ions [5,6] and the larger energies measured for ion pairs [4]. Thus the effect of the momenta of the neutral fragment on the extraction probability can be neglected, and the ion-pair extraction probability calculation can be done assuming a two-body breakup.

In order to evaluate the cross sections of all single-ion and ion-pair breakup channels from the areas measured from Figs. 2 and 3 some corrections have to be made beyond the correction for the different detection efficiencies of the different channels. The main corrections are random coincidences, lost fragments, ^{13}C isotope, and contaminant ions in the target gas. The lost-fragment correction is needed because in some of the events where an ion pair was produced in a single collision, such as $\text{H}_m^+ + \text{CH}_n^+$, only one of the ions was

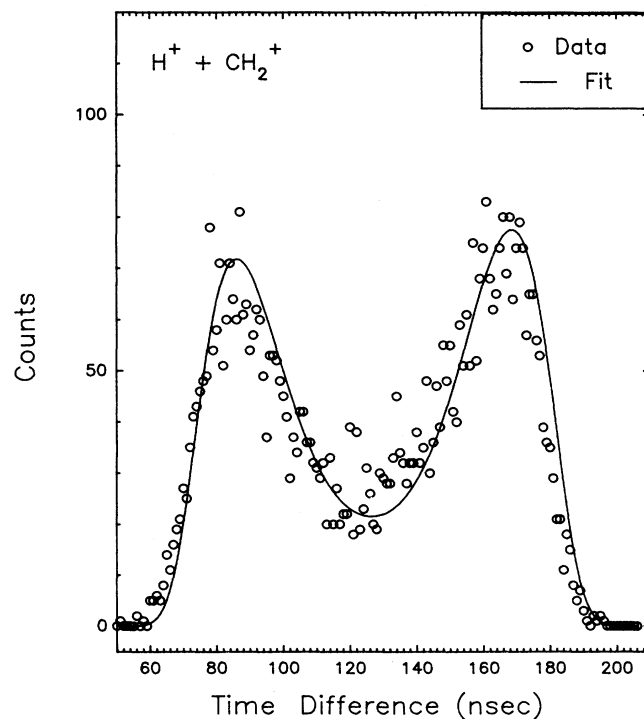


FIG. 4. Time-difference spectrum of the $\text{CH}_4^{2+} \rightarrow \text{H}_2^+ + \text{CH}_2^+$ breakup channel produced by 4-MeV proton impact. The extraction field was 187 V/cm. Data: \circ , simulated spectrum with $\bar{E}_k = 7 \text{ eV}$ and a FWHM of 4 eV, — — —.

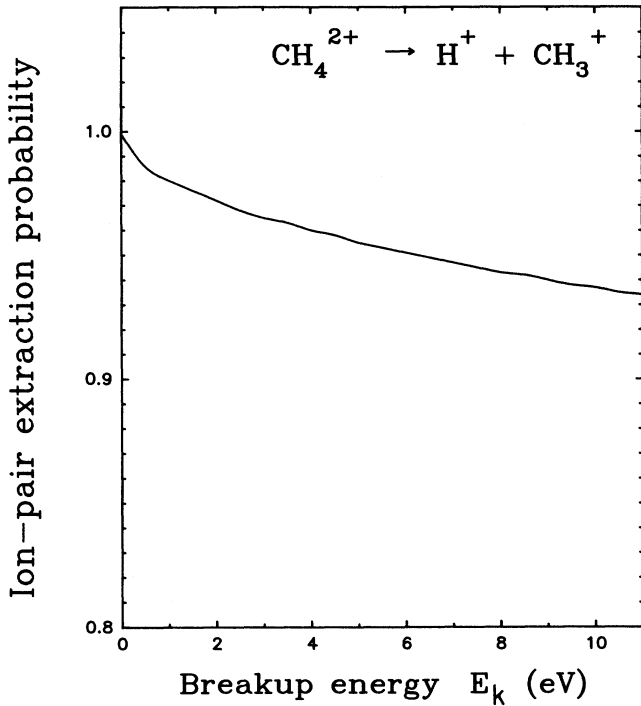


FIG. 5. The ion-pair detection efficiency as a function of the kinetic energy released in the $\text{CH}_4^{2+} \rightarrow \text{H}^+ + \text{CH}_3^+$ breakup.

detected. This effect, for example, is the main contributor to the C^{2+} fragments in the single-ion spectrum as the fragmentation of a CH_4^{2+} into a doubly charged carbon and four neutral hydrogen atoms is very unlikely.

Another important correction is needed because of random coincidences caused by two collisions occurring within the same beam bunch, even though the experiment was performed in single-collision conditions (i.e., a linear pressure dependence of the CH_4^+ count rate). The measured number of random coincidence counts, $C_R^{\text{meas}}(m, n)$, caused by two ion-neutral-fragment channels is given by

$$C_R^{\text{meas}}(m, n) = \tau S^{\text{meas}}(m) S^{\text{meas}}(n), \quad (1)$$

where $S^{\text{meas}}(m)$ and $S^{\text{meas}}(n)$ are the number of counts of the two single channels, and τ is the random coincidence coefficient. This random coincidence coefficient was evaluated directly from the data to be $\bar{\tau} = (2.6 \pm 0.7) \times 10^{-10}$ by using coincidence channels which are purely random, for example, the coincidence of C^+ with CH_4^+ .

The methane target gas used has the natural abundance of ^{13}C (1.1%), thus $^{13}\text{CH}_n^+$ ions have an m/q higher by one unit than the $^{12}\text{CH}_n^+$ ions. This contribution was also included in the data reduction but for clari-

ty it was not included in the yield equations presented in this paper.

Finally, some contaminants in the target gas, mainly N_2 , O_2 , and H_2O , have to be subtracted from both single-ion and coincidence channels. These contaminants were subtracted by measuring proton impact on these targets under the same conditions and normalizing it to the singly charged molecular ions (i.e., H_2O^+ , N_2^+ , and O_2^+). For the clarity of the discussion hereafter the background contribution is not included in the yield equations even though they were included in the data reduction.

As discussed briefly above (and in more detail elsewhere [21,23]) the breakup channels producing one ion and the ones producing ion pairs contribute to counts in both the single-event and coincidence spectra. In order to calculate the true number of events in each breakup channel we have to solve a set of nonlinear coupled equations. The coupling strength depends strongly on the values of η_{mn} , ϵ_r , and $\bar{\tau}$. The equations describing the measured number of singles, for example, the number of CH_n^+ single ions, $S^{\text{meas}}(\text{CH}_n^+)$, are given by

$$S^{\text{meas}}(\text{CH}_n^+) = \epsilon_r S(\text{CH}_n^+) + \sum_m \epsilon_r P_{1\text{of}2}(m, n) \times C(\text{H}_m^+, \text{CH}_n^+), \quad (2)$$

where $S(\text{CH}_n^+)$ is the true number of CH_n^+ single events, $C(\text{H}_m^+, \text{CH}_n^+)$ is the true number of $\text{H}_m^+ + \text{CH}_n^+$ ion-pair events, and $\epsilon_r P_{1\text{of}2}(m, n)$ is the probability of detecting one fragment out of two [23]. Double collision contributions to the single-fragment rates were not included because they are negligible in comparison with the lost-fragment correction. Similar equations describe all the other single-fragment channels measured.

The equations describing the measured number of $\text{H}_m^+ + \text{CH}_n^+$ coincidences, $C^{\text{meas}}(\text{H}_m^+, \text{CH}_n^+)$, are given by

$$C^{\text{meas}}(\text{H}_m^+, \text{CH}_n^+) = \eta_{mn} \epsilon_r^2 C(\text{H}_m^+, \text{CH}_n^+) + \bar{\tau} \epsilon_r^2 S(\text{H}_m^+) S(\text{CH}_n^+). \quad (3)$$

Double collisions which include an ion pair were not included in Eq. (3) because they are negligible relative to the ion-neutral-fragment double collisions and the true rates.

We have also observed ion triplets from the fragmentation of the CH_4^{3+} molecular ion, for example, $\text{CH}_4^{3+} \rightarrow \text{H}^+ + \text{H}_2^+ + \text{CH}^+$. The equations describing the measured number of $\text{H}_k^+ + \text{H}_m^+ + \text{CH}_n^+$ triple coincidences, $T^{\text{meas}}(\text{H}_k^+, \text{H}_m^+, \text{CH}_n^+)$, where $k + n + m \leq 4$, are given by

$$T^{\text{meas}}(\text{H}_k^+, \text{H}_m^+, \text{CH}_n^+) = \eta_{kmn} \epsilon_r^3 T(\text{H}_k^+, \text{H}_m^+, \text{CH}_n^+) + \bar{\tau}_3 \epsilon_r^3 S(\text{H}_k^+) S(\text{H}_m^+) S(\text{CH}_n^+) + \bar{\tau} \epsilon_r^2 [S(\text{H}_k^+) C(\text{H}_m^+, \text{CH}_n^+) + S(\text{H}_m^+) C(\text{H}_k^+, \text{CH}_n^+) + S(\text{CH}_n^+) C(\text{H}_k^+, \text{H}_m^+)], \quad (4)$$

TABLE I. The abundances of all final products from $H^+ + CH_4$ collisions at 4 MeV relative to the CH_4^+ yield (in %).

Ion	Single ions		Ion pairs		Ion triplets
	(%)	$H^+ +$ (%)	$H_2^+ +$ (%)	$H_3^+ +$ (%)	$H^+ + H_2^+ +$ (%)
CH_4^+	100±1				
CH_3^+	84.1±0.8	0.597±0.092			
CH_2^+	12.0±0.2	0.89±0.12	0.23±0.03		
CH^+	3.7±0.1	0.631±0.087	0.018±0.002	0.0020±0.0003	0.0021±0.0006
C^+	0.57±0.06	0.442±0.061	0.011±0.002	0.0002±0.0001	0.0006±0.0002
C^{2+}		0.0152±0.0021	0.0004±0.0002		
H_3^+	0.0048±0.0005	0.0007±0.0002			
H_2^+	0.44±0.04	0.010±0.002			
H^+	7.7±0.4	0.03±0.02			

where τ_3 is the triple random coincidence rate coefficient defined and evaluated in a similar way as the random coincidence coefficient τ given in Eq. (1), and η_{kmn} is the triple-ion extraction probability defined in a similar way as η_{mn} was defined for ion pairs (i.e., the probability that all three ions will make it through the exit collimator). For the strong extraction field used, these extraction probabilities are close to unity, thus $\eta_{kmn} \sim \eta_{mn}$. (Hereafter, we will use $\eta_{kmn} = \eta_{mn}$ for simplicity.) These channels in which the CH_4^{3+} dissociates into three fragments are much smaller than the other breakup channels because triple ionization at this collision velocity is very small. Some of these events will be detected as ion pairs when the third fragment is not detected. This correction to the ion-pair rate was included in the rate equations, but was important only for the $H^+ + H_2^+$ channel.

These sets of nonlinear coupled equations were solved using an iterative method discussed in a previous publication [23] to evaluate the number of single-ion, ion-pair, and ion-triplet events. The abundances evaluated from the true number of events are given in Table I relative to the yield of CH_4^+ . The total cross section for all the fragmentation channels given in Table I can be evaluated using the previously measured [13] total cross section for CH_4^+ production by 4-MeV proton impact, $\sigma = (3.8 \pm 1.1) \times 10^{-17} \text{ cm}^2$.

IV. RESULTS AND DISCUSSION

A. Fragmentation pattern

We have compared the true number of single ions and ion pairs produced by 4-MeV proton impact. In Fig. 6 we have plotted the true number detected, i.e., $\epsilon_r S(n)$ and $\epsilon_r^2 C(m, n)$ and the measured numbers. The single-ion rates are reduced the most for H_m^+ fragments and for channels where many hydrogen fragments have been produced. On the other hand, the main single-ion channels, CH_4^+ and CH_3^+ , are not significantly affected by the lost-fragment correction. The most impressive correction is the total disappearance of the C^{2+} single ions. The C^{2+} ions are produced only in the dissociation of CH_4^{3+} into ion pairs and appear as single ions whenever the other charged ion is not detected. This special

channel can be used to determine a minimum value for the recoil detection efficiency directly as will be discussed elsewhere [25]. The ion-pair rates are less affected by the corrections except for a significant reduction in the $H^+ + CH_3^+$ channel due to the high random coincidence rate contributing to this channel. The correction of this channel is of special importance because all ion pairs were normalized to it in previous studies of CH_4^{2+} fragmentation [4,10,11]. Even though the random coincidence contribution is subtracted, the error in this channel is relatively large and it is better to normalize the ion-pair rates to the ion-pair channels which have a smaller error, such as $H^+ + CH_2^+$, which is the dominant channel, or the $H_2^+ + CH_2^+$ channel, which is a true two-body breakup.

No doubly charged molecular ions of CH_n^{2+} fragments were detected. The peaks at $m/q = 7$ and 8 seen in the single-ion spectrum are associated with N^{2+} and O^{2+} ions from the H_2O , N_2 , and O_2 residual gas. CH_n^{2+} ions have not been seen in double-ionization spectra of CH_4 independent of the ionization mechanism involved, i.e., photoionization [3,4], electron impact [9–11], or proton impact [12,13]. On the other hand, these doubly charged ions have been detected in electron stripping collisions of CH_n^+ on various targets [18–20]. The mean lifetime of the doubly charged ions detected was larger than a microsecond. The typical extraction time of these ions in our system is of the order of 0.1 μsec . Thus we can conclude that all the doubly charged CH_n^{2+} ions produced in $H^+ + CH_4$ collisions decay rapidly into singly charged ion pairs. Gray, Legg, and Needham [16] have shown that these doubly charged ions (and triply charged ions as well) were produced in collisions of 19-MeV F^{4+} ions with CH_4 . In their studies they employed a time-of-flight spectrometer coupled with an energy analyzer, thus having a higher sensitivity to these small multiple ionization channels and short-lived multiply charged ions.

Coincidence time-of-flight studies of molecular fragmentation caused by proton impact ionization is a powerful method as can be seen from the large number of new measured breakup channels of the methane molecule. These channels have such a small abundance that it makes it hard to detect them in photodissociation experiments where the total measured yield is much smaller.

For example, the breakup of CH₄²⁺ into H₃⁺ + CH⁺ was predicted by Siegbahn [17] to be a small breakup channel because the dynamics of the fragmentation favor a breakup of one CH bond leading to a fast emission of one proton.

Another special channel is the production of a proton pair, i.e., CH₄²⁺ → H⁺ + H⁺ + neutral fragments. It is hard to detect this event because of the small time difference between the hits of the two protons (typically

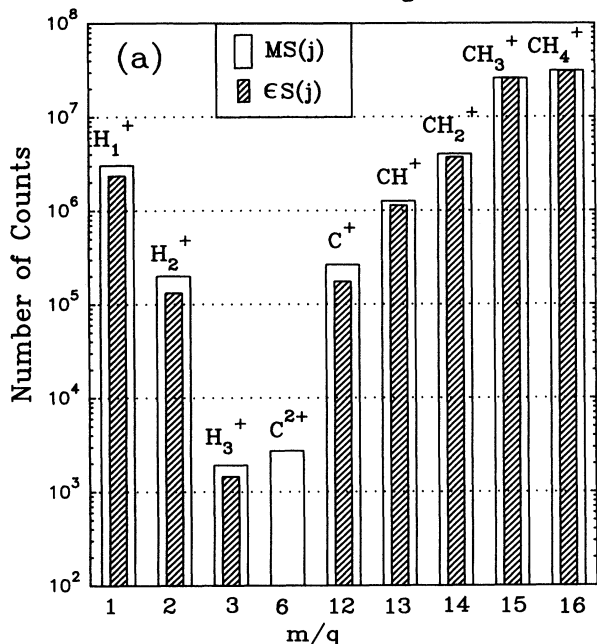
much smaller than the minimum separation time needed by the electronic system). Using a low extraction field some of these events have been detected. This enabled us to approximately determine the relative abundance of this breakup channel. The error associated with it is significantly larger than for other channels due to the large corrections needed to account for the low detection efficiency. The contribution of this ion-pair breakup channel to the H⁺ single-ion production because of lost fragments is negligible because of its very low rate, thus the uncertainty in this channel will not affect the other channels. Further studies of this ion-pair breakup channel are needed using a detection system which can handle simultaneous multiple hits.

The abundance of all recoil ions (i.e., single ions, ion pairs, and ion triplets) relative to the CH₄⁺ molecular ion yield are shown in Table II for different ionization mechanisms (i.e., photoionization, electron impact ionization, proton impact ionization). In most previous measurements the ion pairs were not separated from the ion-neutral-fragment channels, thus a direct comparison of the single-fragment production is impossible. The relative yields of all recoil ions are similar to the single ions, however, because single ionization is two orders of magnitude larger than double ionization. The main feature of the fragmentation pattern of CH₄⁺ is the decrease of the yield of CH_n⁺ ions with increasing number of missing hydrogen fragments. The ratio of CH₃⁺ to CH₄⁺ is practically the same for all ionization mechanisms. On the other hand, the relative differences between the different ionization mechanisms increase with the increasing number of hydrogen fragments produced. It is not clear if the differences are due to the different projectiles or to differences in the impact energy. Further studies at a wide range of impact energy might shed light on this issue.

The abundance of the main ion-pair channels relative to the H⁺ + CH₃⁺ channel is presented in Table III for photoionization, electron impact, and proton impact. Our data are in reasonable agreement with the 10-keV electron impact data even though the collision velocity is significantly different. The 1-keV electron impact data have much smaller relative yields for all channels. The relative abundances for this data set were obtained directly from the number of counts and no corrections were made for efficiency differences or random coincidence rates [10]. We can thus assume that the errors associated with this data set are relatively large. The main product of the fragmentation of the doubly charged methane ion is the three-body breakup CH₄²⁺ → H⁺ + CH₂⁺ + H. This channel has a threshold energy of 33.3 eV, thus it can be produced also by the photoionization process [3]. In that process, however, the probability for removing a few hydrogen atoms is much smaller because the excitation energy of the doubly charged ion is much smaller than the excitation caused by fast-electron or proton impact.

The complete fragmentation pattern of CH₄³⁺ cannot be determined from our measurement because of the low number of counts and the simultaneous multiple hit of the H⁺ fragments. Even though the counting rate was

Measured and Corrected Single Ion Counts



Measured and Corrected Ion-Pair Counts

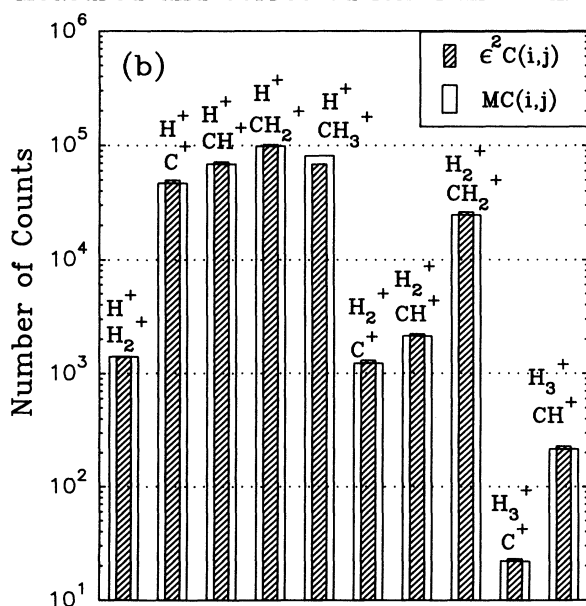


FIG. 6. The measured and true number of ion-neutral and ion-pair events produced in H⁺ + CH₄ collisions at 4 MeV.

TABLE II. The abundances of singles relative to the CH_4^+ yield produced by 4-MeV proton impact dissociation.

Ion	$\text{H}^+ + \text{CH}_4$	$\text{H}^+ + \text{CH}_4$	$\text{H}^+ + \text{CH}_4$	$e^- + \text{CH}_4$	$e^- + \text{CH}_4$	$e^- + \text{CH}_4$	$h\nu + \text{CH}_4$
	(%) 4 MeV This work	(%) 4 MeV Ref. [13]	(%) 2.25 MeV Ref. [12]	(%) 1 keV Ref. [9]	(%) 10 keV Ref. [11]	(%) 1225 eV Ref. [12]	(%) 21.3 eV Ref. [1]
CH_4^+	100±1	100	100	100	100	100	100
CH_3^+	84.7±0.9	82.9±8.3	84	94.7	86	86	70
CH_2^+	13.1±0.3	21.3±6.4	9.7	13.2	11	15.5	4.5
CH^+	4.3±0.1	6.92±2.1	3.1	4.6	3.8	6.3	
C^+	1.02±0.08	1.23±0.37	0.6	1.4		2.0	
H_3^+	0.0077±0.0007						
H_2^+	0.71±0.05			1.1			
H^+	10.3±0.4			6.1	10		

low a few breakup channels have been measured. The dominant breakup channel is $\text{CH}_4^{3+} \rightarrow \text{H}^+ + \text{H}_2^+ + \text{CH}^+$ while the production of a $\text{H}^+ + \text{C}^{2+}$ channel is much less favorable (about 10% of the channels measured). This suggests that multiply charged methane is more likely to break into many singly charged ions than into a highly charged carbon and some neutrals. The complete fragmentation pattern of multiply charged methane can be better studied using fast highly charged projectiles, which are known to have large multiple ionization cross sections. (For example, triple ionization is about 10% of the total ionization of Ne in $\text{F}^{9+} + \text{Ne}$ collisions [26].)

B. Dissociation energy

The distribution of kinetic energy of the single recoil ions produced by electron impact was measured using high-resolution methods [5,6]. The average values of these distributions are of the order of an eV for CH_n^+ and about 2.5 eV for H^+ and H_2^+ ions. The average kinetic energy of each single recoil ion can be evaluated from the width of the single-ion peak in the TOF spectrum measured with a low extraction field. Using a

TABLE III. The abundance of the main ion-pair channels relative to the $\text{H}^+ + \text{CH}_3^+$ yield produced by fast-electron and proton impact dissociation.

Ion pair	$\text{H}^+ + \text{CH}_4$	$e^- + \text{CH}_4$	$e^- + \text{CH}_4$	$h\nu + \text{CH}_4$
	(%) 4 MeV This work	(%) 1 keV Ref. [10]	(%) 10 keV Ref. [11]	(%) 40.8 eV Ref. [4]
$\text{H}^+ + \text{CH}_3^+$	100±10	100	100	100
$\text{H}^+ + \text{CH}_2^+$	149±11	100	142	65
$\text{H}^+ + \text{CH}^+$	106±8	50	97	15
$\text{H}^+ + \text{C}^+$	74±6	30	64	
$\text{H}^+ + \text{C}^{2+}$	2.5±0.2			
$\text{H}^+ + \text{H}_2^+$	1.7±0.2			
$\text{H}_2^+ + \text{CH}_2^+$	38±3	20	32	27
$\text{H}_2^+ + \text{CH}^+$	3.0±0.2			
$\text{H}_2^+ + \text{C}^+$	1.8±0.1			
$\text{H}_3^+ + \text{CH}^+$	0.33±0.04			

method similar to the one described in detail by Levin *et al.* [27] the relationship between the ion energy and the TOF peak width is given by

$$E = \frac{q^2 \mathcal{E}_2^2 (\delta T_{\text{TOF}})^2}{m} \quad (5)$$

where δT_{TOF} is the time difference between the ion moving away from the detector and toward the detector, and q and m are the fragments charge state and mass, respectively. We have used the full width at half maximum (FWHM) as an approximation for δT_{TOF} to evaluate the mean values of the ions' average energies. These results are in general agreement with the more precise electron impact data shown in Table IV. The kinetic energy released in the dissociation can be estimated easily assuming a two-body breakup. The energy of most ion-neutral-fragment breakup channels is very small, of the order of 1–2 eV.

The kinetic energy released in an ion-pair breakup can be measured with a better accuracy by fitting a simulated curve to the time difference spectrum of the breakup channel as shown for $\text{CH}_4^{2+} \rightarrow \text{H}_2^+ + \text{CH}_2^+$ in Fig. 4. Using this method both the average kinetic energy and the width of the distribution can be evaluated. The values obtained for the main ion-pair breakup channels are compared in Table V with photodissociation mea-

TABLE IV. The average kinetic energy of single ions produced by electron and proton impact dissociation. Estimated kinetic energy released in the breakup assuming two-body breakup, i.e., $E_k = E_n(1 + M_n/M_m)$ (using E_n from the first column).

m_i	\bar{E}_n (eV)	\bar{E}_k (eV)	\bar{E}_n (eV)
	Ref. [6]		This work
CH_4^+	0.07	0.07	0.012±0.01
CH_3^+	0.081	1.3	0.02±0.01
CH_2^+	0.268	2.144	0.113±0.05
CH^+	0.296	1.58	0.162±0.05
C^+	0.309	1.236	0.23±0.0
H_3^+			0.50±0.1
H_2^+	2.55	2.91	2.0±0.2
H^+	3.16	3.37	2.4±0.4

TABLE V. The average, E_k , and full width at half maximum (FWHM) of the kinetic-energy release distribution in ion-pair breakup evaluated from the time difference spectrum. The kinetic energy released evaluated as the sum of the individual average energies of both ions, $E'_k = E_m + E_n$. The slopes and correlation coefficients of all ion-pairs plotted in Fig. 7.

Channel	Ref. [4]		This work				
	E_k	FWHM	E_k	FWHM	$E'_k = E_m + E_n$	ρ	Slope
H ⁺ +CH ₃	6	4.5	6.5±1	4±1	7±0.5	-0.924	-0.932
H ⁺ +CH ₂ ⁺	5.1		6±1	4±1	6.7±0.5	-0.863	-0.780
H ⁺ +CH ⁺	5.1		6±1	4±1	7.7±0.5	-0.777	-0.761
H ⁺ +C ⁺			6.5±1	4±1	11.9±0.7	-0.598	-0.818
H ⁺ +C ²⁺						-0.605	-2.282
H ₂ ⁺ +CH ₂ ⁺	6	4.0	7±1	4	7.1±0.4	-0.968	-0.953
H ₂ ⁺ +CH ⁺			6.5±1.5			-0.845	-0.872
H ₂ ⁺ +CH ⁺			6.5±1.5			-0.889	-1.058
H ₃ ⁺ +CH ⁺						-0.929	-0.968

measurements done by Fournier *et al.* [4]. The energies released in the proton impact collisions are slightly larger. This method for evaluating the kinetic energy released in the dissociation is based on the assumption that the process can be treated as a two-body breakup, i.e., the momentum of the neutral fragments is negligible. This was shown to be the case for the photodissociation [3] channel CH₄²⁺ → H⁺ + CH₂⁺ + H. In order to check for deviations from the two-body breakup it is convenient to plot the number of counts as a function of the times of flight of both fragments, t_1 and t_2 . These density plots are shown in Fig. 7 for most of the ion-pair channels. (All times of flight were shifted so that the center of the distribution coincides with the center of the viewing window.) For two-body breakup the times of flight of the two singly charged fragments are related, because of linear momentum conservation, as follows,

$$t_2 = -t_1 + \text{const.} \quad (6)$$

The times of flight of most ion-pair breakup channels shown in Fig. 7 follow this linear dependence. The slope and the correlation coefficient, ρ , between the times of flight of each ion plotted in the figure are presented in Table V. They are both ~ -1 for the true two-body breakup channels, H⁺+CH₃⁺, H₂⁺+CH₂⁺, and H₃⁺+CH⁺, as expected. Both the slope and the correlation coefficient decrease with the increasing number of neutral hydrogen atoms produced, but the deviations from linearity are not too large to affect the evaluation of the ion-pair extraction probability discussed in the previous section. The most significant deviations from linearity occur for the H⁺+CH⁺ and H⁺+C⁺ channels. Thus, using the time-difference spectrum to evaluate their kinetic-energy release is not expected to be as good as for the channels which fulfill this condition. The energy released can also be evaluated in a way similar to the method used for the single ions by measuring the TOF peak widths of each ion separately (i.e., the widths of the projections onto the t_1 and t_2 coordinates of Fig. 7). These energies $E'_k = E_m + E_n$, shown in Table V, are in agreement with the energies evaluated using the time-difference spectrum for most channels but are significantly higher for the H⁺+C⁺ breakup channel.

The higher values of E'_k have been used to determine the ion-pair extraction probability for these channels. In general, the kinetic energy of the ion pairs is about 6–7 eV while the ion-neutral-fragment kinetic energy is about 1–2 eV.

C. Dissociation pathways

The relative abundance and the kinetic energy released in most ion-pair breakup channels have been determined. This information can be used in an attempt to determine

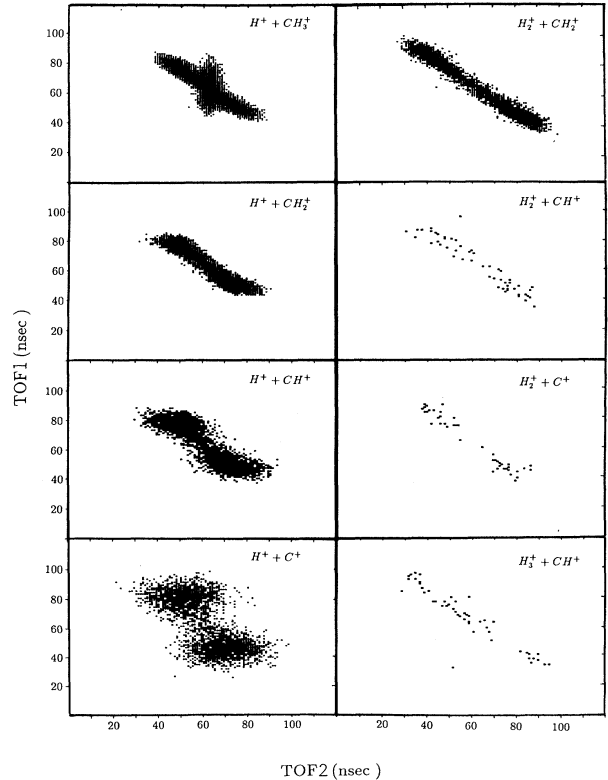
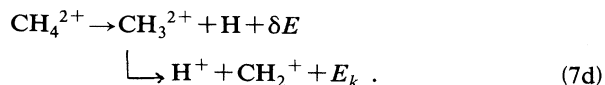
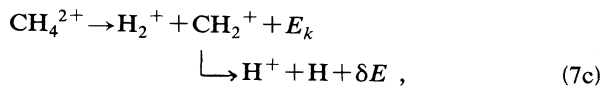
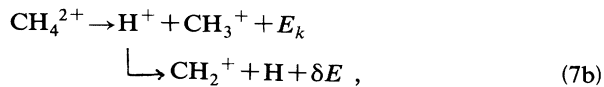
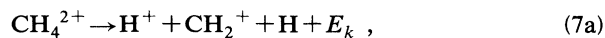


FIG. 7. The time-of-flight spectra of the main ion-pair breakup channels, produced by 4-MeV proton impact. Plotted as a density plot of intensity as a function of TOF₁ and TOF₂.

the possible pathways of breakup of the CH_4^{2+} into the final products. For example, one should consider the following pathways for the production of $\text{H}^+ + \text{CH}_2^+ + \text{H}$:



The first mechanism is the direct breakup into three fragments while the other three are two-step mechanisms. From the dissociation energy data discussed in the previous subsection, it is reasonable to assume that for two-step breakup the energy released in the ion-neutral-fragment breakup step δE is much smaller than the energy released in the ion-pair breakup step E_k . (This assumption is equivalent to the assumption that the neutral fragment has negligible momentum.) Using linear momentum conservation in the ion-pair breakup and neglecting δE the ratio of kinetic energy of both ions can be evaluated. For example, for the pathway given in Eq. (7b) the energy ratio is

$$\begin{aligned} \frac{E_k(\text{CH}_2^+)}{E_k(\text{H}^+)} &= \frac{\frac{14}{15}E_k/(1+15/1)}{E_k/(1+1/15)} \\ &= \frac{14}{15} \frac{(1+1/15)}{(1+15)} = 0.062, \end{aligned} \quad (8)$$

where the factor of $\frac{14}{15}$ comes from the second step where the CH_3^+ dissociates into $\text{CH}_2^+ + \text{H}$, both having approximately the same speed. The ratios $E_k(\text{CH}_n^+)/E_k(\text{H}_m^+)$, calculated using this simple breakup model are presented in Table VI. The two-step mechanism in which the H_m^+ fragments further dissociate yields ratios which are too high in comparison with the experimental values. Thus this pathway is not a dominant one. The last pathway given in Eq. (7d) yields the same ratios as the direct pathway but it requires the formation of metastable doubly charged molecular ions in order to allow the slow hydrogen atom to get away from

the molecule center of gravity before the fast H^+ will be released. Even though this pathway is not excluded by our data it is not expected to dominate because these long-lived molecular ions are not easily produced. To conclude, the most likely pathways of formation of the main final products are either the direct breakup or the two-step mechanism in which first a $\text{H}_m^+ + \text{CH}_n^+$ ($m+n=4$) is produced and then the CH_n^+ further dissociates into an ion-neutral-fragment pair. In both pathways most of the H_m^+ formed in the collision is detected before further dissociation takes place. The relative abundance of breakup channels in which a H_m^+ was formed decreases rapidly with increasing m , in agreement with the theoretical prediction by Siegbahn [17]. The assignment of the pathway leading to the final ion-pair products of the dissociation of CH_4^{2+} might be improved by determining the linear momentum of each ion in addition to their kinetic energy. This can be done using a position sensitive detector as explained for example by Cheng *et al.* [28]. A more detailed theoretical description of the fragmentation dynamics is needed in order to compare quantitatively the relative rates of the different breakup channels and to determine the preferred pathway.

V. CONCLUSIONS

Molecular fragmentation of methane induced by 4-MeV proton impact has been investigated using the coincidence time-of-flight spectroscopy technique. In these collisions, mostly singly charged CH_4^{+*} molecular ions are produced. Most of these molecular ions are unstable and rapidly dissociate into an ion-neutral-fragment pair releasing a kinetic energy of less than 1 eV for CH_n^+ , and about 2.5 eV for H^+ and H_2^+ . The abundance of the single ions relative to CH_4^+ is similar to the ones measured previously for photodissociation and electron and proton impact. The doubly charged molecular ion, CH_4^{2+} , dissociates rapidly into an ion pair. The abundance of the main ion-pair channels relative to $\text{H}^+ + \text{CH}_3^+$ is in good agreement with the 10-keV electron impact data. On the other hand, photodissociation and 1-keV electron impact tend to be less efficient in producing many hydrogen fragments. The method used allowed us to measure a few breakup channels of CH_4^{2+} which have not been seen before, including the small breakup channel $\text{H}_3^+ + \text{CH}^+$. Our data for CH_4^{2+} breakup are consistent with either a direct production of

TABLE VI. The ratio of kinetic energies of both ions in an ion-pair breakup calculated for the different pathways (see text) and the experimental ratio.

Final product	$E(\text{CH}_n^+)/E(\text{CH}_m^+)$				Experiment
	$\text{H}_m^+ + \text{CH}_n^+$ Direct (7a),(7d)	$\text{H}^+ + \text{CH}_3^+$ Two step (7b)	$\text{H}_2^+ + \text{CH}_2^+$ Two step (7c)	$\text{H}_3^+ + \text{CH}^+$ Two step (7c)	
$\text{H}^+ + \text{CH}_3^+$	0.067	0.067			0.064 ± 0.006
$\text{H}^+ + \text{CH}_2^+$	0.071	0.062	0.286		0.074 ± 0.009
$\text{H}^+ + \text{CH}^+$	0.077	0.058	0.265	0.692	0.089 ± 0.012
$\text{H}^+ + \text{C}^+$	0.083	0.053	0.245	0.639	0.054 ± 0.005
$\text{H}_2^+ + \text{CH}_2^+$	0.143				0.156 ± 0.012

all fragments or a two-step mechanism, in which a fast two-body breakup into H_m⁺ and a CH_n⁺ occurs first, where the number of hydrogen atoms on the light fragment, *m*, is also the number of CH bonds broken simultaneously. Later the CH_n⁺ fragment further dissociates by emitting very slow hydrogen atoms.

ACKNOWLEDGMENTS

We wish to thank Professor T. Gray for many useful discussions. This work was supported by the Office of Basic Energy Sciences, U.S. Department of Energy. D.T.J. and P.J.N. were partly supported by the National Science Foundation.

-
- [1] B. Brehm and E. V. Puttkamer, *Z. Naturforsch. Teil A* **22**, 8 (1967).
- [2] J. H. D. Eland, *Mol. Phys.* **61**, 725 (1987), and references therein.
- [3] G. Dujardin, D. Winkoun, and S. Leach, *Phys. Rev. A* **31**, 3027 (1985), and references therein.
- [4] P. G. Fournier, J. Fournier, F. Salama, P. J. Richardson, and J. H. D. Eland, *J. Chem. Phys.* **83**, 241 (1985).
- [5] J. Appell and C. Kubach, *Chem. Phys. Lett.* **11**, 486 (1971).
- [6] Von R. Fuchs and R. Taubert, *Z. Naturforsch. Teil A* **19**, 494 (1964).
- [7] H. H. Chatham, D. Hils, R. Robertson, and A. Gallagher, *J. Chem. Phys.* **81**, 1770 (1984).
- [8] O. J. Orient and S. K. Srivastava, *J. Phys. B* **20**, 3923 (1987).
- [9] B. Adamczyk, A. J. H. Boerboom, B. L. Schram, and J. Kistemaker, *J. Chem. Phys.* **44**, 4640 (1966).
- [10] K. E. McCulloh, T. E. Sharp, and H. M. Rosenstock, *J. Chem. Phys.* **42**, 3501 (1965).
- [11] C. Backx and M. J. Van der Weil, *J. Phys. B* **8**, 3020 (1975).
- [12] S. Wexler, *J. Chem. Phys.* **41**, 2781 (1964).
- [13] N. B. Malhi, I. Ben-Itzhak, T. J. Gray, J. C. Legg, V. Needham, K. Carnes, and J. H. McGuire, *J. Chem. Phys.* **87**, 6502 (1987).
- [14] R. J. Maurer, C. Can, and R. L. Watson, *Nucl. Instrum. Methods Phys. Res., Sect. B* **27**, 512 (1987).
- [15] H. Tawara, T. Tonuma, H. Kumagai, and T. Matsuo, *Physica Scr.* **42**, 434 (1990), and references therein.
- [16] T. J. Gray, J. C. Legg, and V. Needham, *Nucl. Instrum. Methods Phys. Res., Sect. B* **10/11**, 253 (1985).
- [17] Per E. M. Siegbahn, *Chem. Phys.* **66**, 443 (1982).
- [18] T. Ast, C. J. Porter, C. J. Proctor, and J. H. Beynon, *Chem. Phys. Lett.* **78**, 439 (1981).
- [19] M. Rebrenovic, A. G. Brenton, and J. H. Beynon, *Int. J. Mass Spectrom. Ion Phys.* **52**, 1175 (1983).
- [20] D. Mathur and C. Badrinathan, *J. Phys. B* **20**, 1517 (1987), and references therein.
- [21] I. Ben-Itzhak, S. G. Ginther, and K. Carnes, *Nucl. Instrum. Methods Phys. Res., Sect. B* **66**, 401 (1992).
- [22] H. Knudsen, L. H. Andersen, P. Hvelplund, G. Astner, H. Cederquist, H. Danared, L. Liljeby, and K.-G. Rensfelt, *J. Phys. B* **17**, 3545 (1984).
- [23] I. Ben-Itzhak, S. G. Ginther, and K. D. Carnes, *Phys. Rev. A* **47**, 2827 (1993).
- [24] G. Sampoll, R. L. Watson, O. Heber, V. Horvat, K. Wohrer, and M. Chabot, *Phys. Rev. A* **45**, 2903 (1992), and references therein.
- [25] I. Ben-Itzhak, S. G. Ginther, and K. D. Carnes, *Nucl. Instrum. Methods (to be published)*.
- [26] T. J. Gray, C. L. Cocke, and E. Justiniano, *Phys. Rev. A* **22**, 849 (1980).
- [27] J. C. Levin, H. Cederquist, R. T. Short, I. A. Sellin, L. Liljeby, S. Hultdt, S.-E. Johansson, E. Nilsson, and D. A. Church, *Nucl. Instrum. Methods Phys. Res., Sect. A* **262**, 106 (1987).
- [28] S. Cheng, C. L. Cocke, V. Frohne, E. Y. Kamber, and S. L. Varghese, *Nucl. Instrum. Methods Phys. Res., Sect. B* **56/57**, 78 (1991).